

# NMR Structural Analysis of Cadmium Sensing by Winged Helix Repressor CmtR<sup>\*S</sup>

Received for publication, February 6, 2007, and in revised form, June 21, 2007. Published, JBC Papers in Press, June 27, 2007, DOI 10.1074/jbc.M701119200

Lucia Banci<sup>‡</sup>, Ivano Bertini<sup>†1</sup>, Francesca Cantini<sup>‡</sup>, Simone Ciofi-Baffoni<sup>‡</sup>, Jennifer S. Cavet<sup>§</sup>, Christopher Dennison<sup>¶</sup>, Alison I. Graham<sup>¶</sup>, Duncan R. Harvie<sup>¶</sup>, and Nigel J. Robinson<sup>¶</sup>

From the <sup>‡</sup>Department of Chemistry and Centro Risonanze Magnetiche, University of Florence, Via Luigi Sacconi 6, Florence 50019, Italy, the <sup>¶</sup>Institute of Cell and Molecular Biosciences, Medical School, University of Newcastle, Newcastle NE2 4HH, United Kingdom, and the <sup>§</sup>Department of Life Sciences, University of Manchester, Manchester M13 9PT, United Kingdom

CmtR from *Mycobacterium tuberculosis* is a winged helical DNA-binding repressor of the ArsR-SmtB metal-sensing family that senses cadmium and lead. Cadmium-CmtR is a dimer with the metal bound to Cys-102 from the C-terminal region of one subunit and two Cys associated with helix  $\alpha$ R from the other subunit, forming a symmetrical pair of cadmium-binding sites. This is a significant novelty in the ArsR-SmtB family. The structure of the dimer could be solved at 312 K. The apoprotein at the same temperature is still a dimer, but it experiences a large conformational exchange at the dimer interface and within each monomer. This is monitored by an overall decrease of the number of nuclear Overhauser effects and by an increase of H<sub>2</sub>O-D<sub>2</sub>O exchange rates, especially at the dimeric interface, in the apo form with respect to the cadmium-bound state. The C-terminal tail region is completely unstructured in both apo and cadmium forms but becomes less mobile in the cadmium-bound protein due to the recruitment of Cys-102 as a metal-ligand. DNA binds to the apo dimer with a ratio 1:3 at millimolar concentration. Addition of cadmium to the apo-CmtR-DNA complex causes DNA detachment, restoring the NMR spectrum of free cadmium-CmtR. Cadmium binding across the dimer interface impairs DNA association by excluding the apo-conformers suited to bind DNA.

Life depends on multiple metals (1). Iron-, copper-, and zinc-responsive transcriptional regulators are known in yeast (AFT1, MAC1, ACE1, and ZAP1) (2) and higher eukaryotes (MTF1) (3, 4). In bacteria, multiple families of metal-responsive transcriptional regulators have been described, including ArsR/SmtB-like DNA-binding repressors (5–8). These are a subgroup of winged helix repressors. We previously discovered the cellular zinc sensor SmtB (5). In elevated zinc, SmtB repression of the *smtA* gene is alleviated to allow transcription of a metal-

lothionein gene encoding a protein, which sequesters the surplus metal atoms (9, 10). In contrast, the related ArsR sensor responds to arsenite to regulate production of an arsenical-translocating ATPase (6). The location of the metal-sensing site, the complement of ligands and site geometry, vary in different members of this family of regulators (8, 11–20). There is considerable interest in understanding how metal binding to metal sensors is transduced into altered levels of transcription of their target genes.

*Mycobacterium tuberculosis* contains ten genes encoding ArsR/SmtB sensors making it a useful model organism for studies of these regulators. It is plausible that fluctuations in metal concentrations within macrophages have selected for multiple genes encoding such regulators in this pathogen. One of the *M. tuberculosis* sensors, CmtR, was chosen for structural and functional studies of a sensory mechanism. We previously established that CmtR responds *in vivo* to cadmium and lead to modulate production of a toxic metal-exporting P<sub>1</sub>-type ATPase (16). Residues Cys-57 and Cys-61 plus Cys-102 have been implicated in cadmium perception by a combination of *in vivo* and *in vitro* studies (16, 21). CmtR has a relatively weak affinity for DNA, in the region of 10<sup>-7</sup> M, even in the apo form (22). Here we report a solution NMR investigation of both the demetallated and metallated proteins. We show that the former has a tertiary and quaternary structure that is fluxional, whereas the latter has a more rigid conformation with implications for the metal-sensing mechanism. This is a typical example of a system, which can be tackled by NMR as mobile proteins generally do not crystallize or do so via selection of a single conformer. Additionally, we visualize cadmium inhibition of CmtR DNA binding by NMR.

## MATERIALS AND METHODS

**CmtR Expression and Purification**— $\beta$ -Galactosidase activity was measured in *Mycobacterium smegmatis* mc<sup>2</sup>155 cells containing *cmtR*, or derivatives with codon substitutions at Cys-57, Cys-61, Cys-102, Asp-79, or His-81, fused to *lacZ* in pJEM15 (16). Cells were grown at 37 °C with shaking in LB medium containing 0.05% Tween 80 (v/v) and supplemented with CdCl<sub>2</sub> up to maximum non-inhibitory concentrations (7.5  $\mu$ M) for 20 h immediately prior to assay. Assays were performed in triplicate on at least three separate occasions.

CmtR was expressed for purification as previously described (16). Crude cell lysates were applied to a Heparin affinity column pre-equilibrated in buffer A (10 mM Hepes, 50 mM NaCl, 1

\* This work was supported by a research grant and Ph.D. studentship from the Biotechnology and Biological Sciences and Research Council in European Commission as Contract 031220, SPINE2-COMPLEXES. The costs of publication of this article were defrayed in part by the payment of page charges. This article must therefore be hereby marked "advertisement" in accordance with 18 U.S.C. Section 1734 solely to indicate this fact.

The atomic coordinates and structure factors (code 2JSC) have been deposited in the Protein Data Bank, Research Collaboratory for Structural Bioinformatics, Rutgers University, New Brunswick, NJ (<http://www.rcsb.org/>).

<sup>§</sup> The on-line version of this article (available at <http://www.jbc.org/>) contains supplemental Figs. S1–S7 and Tables S1–S6.

<sup>1</sup> To whom correspondence should be addressed: Tel.: 39-055-457-4272; Fax: 39-055-457-4271; E-mail: ivanobertini@cerm.unifi.it.

mM EDTA, 1 mM dithiothreitol). Bound proteins were eluted using a linear gradient to 1 M NaCl in the same buffer. Fractions containing CmtR were loaded onto a Superdex-75 size-exclusion column equilibrated in buffer A plus 200 mM NaCl. CmtR-containing fractions were pooled and diluted to reduce salt concentration before a single concentration step on a second heparin affinity column. Protein was judged to be >95% pure by SDS-PAGE. For production of dual-labeled CmtR for NMR analysis, *Escherichia coli* BL21 harboring the pET-CmtR expression plasmid, was cultured in M9 minimal media (22). D-Glucose- $^{13}\text{C}_6$  and ammonium- $^{15}\text{N}$  chloride were used. Cultures were grown until  $A_{595} = 0.6$ , and expression was induced by addition of isopropyl 1-thio- $\beta$ -D-galactopyranoside to a final concentration of 0.5 mM for 6.5 h. Labeled CmtR was purified and concentrated as described for unlabeled protein.

Prior to use in experiments, CmtR was desalted by multiple passages through a PD-10 column filled with Sephadex G-25 resin and equilibrated in the required buffer. Protein concentration was calculated using the theoretical extinction coefficient (at 280 nm) of  $4,400 \text{ M}^{-1} \text{ cm}^{-1}$ .

**Mass Spectrometry**—CmtR was desalted into 10 mM ammonium acetate buffer (pH 6.0). 3-fold excess cadmium was added as required. Mass spectroscopy was carried out on a Thermo Finnigan LTQ-MS. Protein was present at  $\sim 5 \text{ pmol } \mu\text{l}^{-1}$ .

**Spectral Analysis of CmtR Metal Binding**—Purified protein was desalted into 10 mM Hepes (pH 7.4), 250 mM KCl buffer in an anaerobic environment. Protein was diluted to the required concentration and sealed in a gas-tight quartz cuvette. Spectra were measured from 200 to 800 nm on a Cary 4E spectrophotometer. Metals were added to the indicated concentrations using a gas-tight Hamilton syringe, allowed to equilibrate for 60 s before reading the spectra.

**NMR Structural and Dynamic Characterization**—In the NMR samples, the final protein concentration ranges between 0.5 and 1 mM. NMR samples also contained 10% v/v  $^2\text{H}_2\text{O}$  for NMR spectrometer lock. The NMR spectra were acquired on  $^{15}\text{N}$ - and  $^{13}\text{C}$ ,  $^{15}\text{N}$ -labeled apo-CmtR and cadmium-CmtR samples at 298 K and 312 K on Avance 800 and 500 Bruker spectrometers equipped with triple resonance Cryoprobes<sup>TM</sup>. The NMR experiments of cadmium- and apo-CmtR, used for the backbone and the aliphatic side-chain resonance assignment and for obtaining structural restraints, are summarized in supplemental Tables S1 and S2, respectively. Resonance assignments of cadmium- and apo-CmtR have been deposited in the BioMagResBank data base and are also reported with details in supplemental Tables S3 and S4. The protonation state of His-81 was determined through  $^2\text{J } ^1\text{H}-^{15}\text{N}$  HSQC<sup>2</sup> experiments (23). Secondary structure elements of apo- and cadmium-CmtR were determined from chemical shift index analysis on  $\text{H}\alpha$ , CO,  $\text{C}\alpha$ , and  $\text{C}\beta$  resonances,  $^3\text{J}_{\text{HNH}\alpha}$  coupling constants,  $d_{\alpha\text{N}}(i-1, i)/d_{\text{N}\alpha}(i, i)$  ratios (24), and NOE patterns.

Structure calculations were performed using the program CYANA 2.1 (25). The CANDID module of CYANA was used for automated assignment of the NOESY cross-peaks, followed

by a manual check prior to the final calculations. All the details for structure calculations of the monomer and of the dimer are reported in supplemental Table S5, which also reports the statistical and quality analysis of the water-energy-minimized structures of cadmium-CmtR. By analyzing three-dimensional  $^{15}\text{N}$ -edited and  $^{13}\text{C}$ -edited NOESY spectra and two-dimensional NOESY spectra, 3056 intra-subunit NOE cross-peaks are assigned and transformed into 2445 unique upper distance limits, of which 1809 are meaningful. The average number of meaningful NOEs per residue is 16.

The presence of 34 NOEs, inconsistent with proton couplings of residues of the same subunit, were identified and assigned to intersubunit couplings (supplemental Table S6) and introduced in the dimeric structure calculations. Distance and dihedral angle restraints and proton pairs stereospecifically assigned were duplicated for each subunit in the dimer structure calculations. To improve the treatment of symmetric dimer structures we have used new types of restraints that have been recently introduced in the program CYANA 2.1, *i.e.* identity restraints and symmetry restraints (25). Cadmium was included in the calculations by adding a chain of dummy atoms to the amino acid sequence that have their van der Waals radii set to 0 with the end one atom having a radius of 1.4 Å, which mimics a cadmium ion. The sulfur atoms of the Cys ligands were linked to the metal ion through upper distance limits of 2.3 Å. Structure calculations were performed by first considering the sulfurs of Cys-57 and Cys-61 as metal donor atoms and then including a third sulfur deriving from Cys-102. When Cys-102 comes from the same subunit, the target function drastically increases, whereas when Cys-102 is absent or provided by the other subunit, the target function does not change. Therefore, the third Cys ligand must exclusively come from the C-terminal tail of the adjacent subunit.

The thirty conformers with the lowest residual CYANA target function values, out of 300 starting conformers used in this final calculation, were restrained energy-minimized using the AMBER 8 package.<sup>3</sup> The force field parameters for the cadmium ion were adapted from those already reported for similar cadmium sites in cadmium proteins (27). The quality of the structure was evaluated in terms of deviations from ideal bond lengths and bond angles and through Ramachandran plots obtained using the programs PROCHECK-NMR and WHAT IF (28, 29). The solution structure of cadmium-CmtR has been deposited in the PDB (2JSC).

$^{15}\text{N}$   $R_1$ ,  $R_2$ , and steady-state heteronuclear  $^{15}\text{N}\{^1\text{H}\}$  NOEs, which can provide information on internal mobility as well as on the overall protein tumbling rate, were measured with pulse sequences described (30) on both apo-CmtR and cadmium-CmtR samples. In all experiments the water signal was suppressed with the “water flipback” scheme (31). The experimental relaxation rates were used to map the spectral density function values,  $J(\omega_H)$ ,  $J(\omega_N)$ , and  $J(0)$ , as described elsewhere

<sup>2</sup> The abbreviations used are: HSQC, heteronuclear single quantum coherence; NOE, nuclear Overhauser effect; NOESY, nuclear Overhauser effect spectroscopy.

<sup>3</sup> D. A. Case, T. A. Darden, T. E. Cheatham, C. L. Simmerling, J. Wang, R. E. Duke, R. Luo, K. M. Merz, B. Wang, D. A. Pearlman, M. Crowley, S. Brozell, V. Tsui, H. Gohlke, J. Mongan, V. Hornak, G. Cui, P. Beroza, C. E. Schafmeister, J. W. Caldwell, W. S. Ross, and P. A. Kollman (2004) AMBER 8. (version 8.0) University of California, San Francisco, CA.

(32). The overall rotational correlation time ( $\tau_m$ ) values were estimated from the  $R_2/R_1$  ratio. In this analysis, care was taken to remove from the input relaxation data those amide protons having an exchange contribution to the  $R_2$  value or exhibiting large-amplitude internal motions on a time scale longer than a few hundred picoseconds as inclusion of these data would bias the calculated  $\tau_m$  value (33).

The kinetics of  $H_2O$ - $D_2O$  exchange were performed diluting concentrated apo- and cadmium-CmtR proteins rapidly with  $^2H_2O$  to a final concentration of 92% (v/v). Hydrogen/deuterium exchange rates were investigated through a series of  $^1H$ - $^{15}N$  HSQC experiments performed over 24 h.

**Interaction of CmtR-DNA Complexes with Metals**—Complementary oligonucleotides corresponding to the previously determined CmtR-binding site (5'-GCTGTTATACCAGTATATGGTGTACTATTTGATCT-3') were synthesized. Oligonucleotides were annealed, resuspended in  $H_2O$ , and subjected to ultracentrifugation in an Airfuge prior to use. The protein-DNA interaction was followed by NMR applying  $^1H$ - $^{15}N$  TROSY and CRINEPT techniques (34). First, the DNA fragment was stepwise added to a solution of 0.1 mM dimeric  $^{15}N$  apo-CmtR in 50 mM phosphate (pH 7) and 0.4 M NaCl buffer. The final dimeric protein:DNA ratio was 3:1 with 1 mM dithiothreitol. An aqueous solution of  $CdCl_2$  was then stepwise added to the DNA-protein mixture up to 1:1 metal:dimeric protein ratio. Second, the DNA fragment was stepwise added to a solution of 0.15 mM dimeric  $^{15}N$  cadmium-CmtR in 50 mM phosphate (pH 7) and 0.4 M NaCl buffer. The final dimeric protein:DNA ratio was 1:3 with 1 mM dithiothreitol.

## RESULTS

**Protein Characterization**—CmtR is a cadmium-detecting transcriptional repressor of 118 residues with a molecular mass of 12.5 kDa that forms homodimers (21). IC-mass spectrometry shows that cadmium-CmtR has a mass of 25,211 under native conditions with volatile buffers, matching a dimer plus two cadmium atoms. The far-UV CD spectra of apo- and cadmium-CmtR have features characteristic of a folded protein with a large content of  $\alpha$ -helices, as indicated by two negative bands at 222 and 209 nm. The peak intensity as well as the overall shape of the CD spectrum of apo-CmtR does not change upon addition of 1 equivalent of  $CdCl_2$  per monomer, indicating that the binding of metal does not affect the content of secondary structure. The  $^1H$ - $^{15}N$  HSQC spectra of apo- and cadmium-CmtR recorded at 298 K are indicative of an essentially folded protein with well dispersed amide signals. However, at this temperature only 60 and 80 NH signals for apo- and cadmium-CmtR, respectively, *versus* 114 expected resonances, were observed. Moreover, the majority of the detected signals were too broad to proceed with a high resolution structure determination. By increasing the temperature to 312 K, the NH signals significantly narrowed in both apo- and cadmium-CmtR (supplemental Figs. S1 and S2), and the number of detected NH signals increased to 89 and 97, respectively. The missing amide resonances are essentially located in the N-terminal region. The overall molecular tumbling rates ( $14.4 \pm 1.7$  ns for apo-CmtR and  $14.9 \pm 1.3$  ns for cadmium-CmtR, respectively, at 312 K) as obtained from  $^{15}N$  relaxation measurements (supplemental

Figs. S3 and S4) show that the protein in solution is in a dimeric state both with and without the metal ion. The  $^{15}N$  relaxation measurements do not show evidence of any conformational equilibria, because they can be revealed only at rates smaller than  $10^5 s^{-1}$ . However, evidence of conformational line-broadening occurs at 298 K as the number of peaks increase with increasing temperature. Only one set of resonances was observed in the NMR spectra of both apo- and cadmium-CmtR, indicating that dimer subunits interact on average in a symmetric way to produce degenerate resonances for both molecules.

**Solution Structure of Cadmium-CmtR**—The solution structure of cadmium-CmtR was solved using 2445 unique upper distance limits obtained from three-dimensional  $^{15}N$ -edited and  $^{13}C$ -edited NOESY spectra and two-dimensional NOESY spectra. Each subunit of the symmetric dimer is composed of five  $\alpha$ -helices (residues 12–18, 21–32, 39–44, 49–61, and 79–87) and a two-stranded  $\beta$ -sheet (residues 63–68 and 73–77) arranged into an  $\alpha 1$ - $\alpha 2$ - $\alpha 3$ - $\alpha R$ - $\beta 1$ - $\beta 2$ - $\alpha 5$ -fold (where  $\alpha R$  represents the DNA recognition helix, following the notation used for SmtB) (Fig. 1A) with similarity to the global folds of SmtB, CzrA, and CadC (13, 17, 18). Helices  $\alpha 3$  and  $\alpha R$  (segments 39–44 and 49–61) form the standard helix-turn-helix motif found in many DNA-binding proteins (35). The other three helices are involved in several hydrophobic interactions within each monomer and serve primarily as a scaffold that orients the helix-turn-helix motif. Furthermore, helices  $\alpha 1$  and  $\alpha 5$  form hydrophobic interactions at the dimer interface. The structure is well defined over the whole sequence (supplemental Fig. S5) with the exception of the C- and N-terminal regions, the latter of which is a consequence of the lack of the detection of resonances for the first ten amino acids. The NH cross-peaks of the C-terminal region (residues 106–118) are all clustered in the typical spectral region of unstructured proteins and are highly flexible, displaying backbone mobility in the nanosecond to picosecond time scale, considerably faster than the overall protein tumbling rate (supplemental Fig. S4). Consequently this region is characterized by a very low number of long range NOEs (supplemental Fig. S5).

A total of 34 unambiguously assigned intersubunit NOEs per chain, mainly involving helices  $\alpha 1$  and  $\alpha 5$ , define the dimeric interface in cadmium-CmtR and unambiguously orient the CmtR subunits in dimer structure calculations (Figs. 1A and 2A). Helices  $\alpha 1$  and  $\alpha 5$  are adjacent and antiparallel to the corresponding helices from the other subunit. The cadmium-CmtR structure shows that Cys-57 and Cys-61 are on helix  $\alpha R$  and in the following loop, respectively, in an appropriate conformation to bind the cadmium ion. The backbone chemical shift changes between apo- and cadmium-CmtR reveals four regions affected by cadmium-binding; (i)  $\alpha 1$  plus the following loop and (ii)  $\alpha 5$  helices, all at the dimer interface, (iii) part of  $\alpha R$ , including Cys-57 and Cys-61, and (iv) the segment 97–102 containing Cys-102 (Fig. 2B).  $^{13}C\alpha$  and  $^{13}C\beta$  chemical shifts of cysteines 57, 61, and 102 are the most affected by cadmium binding, with the chemical shift differences ranging from 1.3 to 5.0 ppm for  $^{13}C\alpha$  and from 1.2 to 3.0 ppm for the  $^{13}C\beta$ . Cadmium binding also reduces the backbone flexibility of the region containing Cys-102 (see later). All of these data are therefore in agreement with direct participation of Cys-102 in

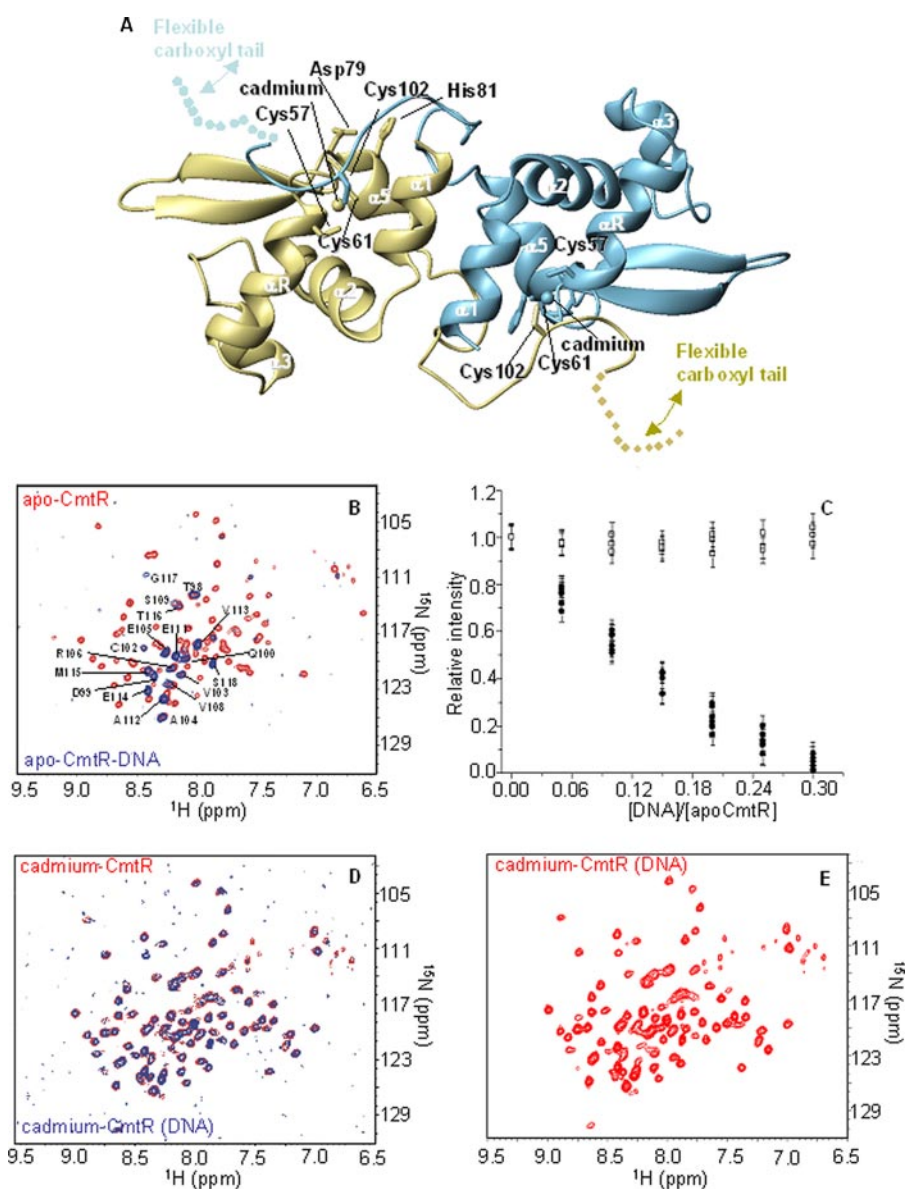


**FIGURE 1. Solution structure of cadmium-CmtR and interaction with DNA.** *A*, ribbon representation of dimeric cadmium-CmtR. One CmtR subunit is beige and the other sky blue (residues 10–106 are shown). Closed circles represent the flexible tail residues 106–118. *B*, the interaction of CmtR with DNA analyzed using  $^1\text{H}$ - $^{15}\text{N}$  HSQC spectra showing apo-CmtR (red) superimposed with apo-CmtR in the presence of DNA (blue). *C*, the intensities of the signals of selected backbone amide groups of apo-CmtR are plotted against the DNA/dimeric apo-CmtR ratio. The figure reports the behavior of residues belonging to both the structured region (filled symbols) and to the unstructured C-terminal region (open symbols). For each residue, all intensities have been scaled relative to the intensity observed in the absence of DNA. *D*,  $^1\text{H}$ - $^{15}\text{N}$  HSQC spectrum of cadmium-CmtR (red) superimposed with that of the dimeric apo-CmtR/DNA 3:1 mixture after the addition of 1 equivalent of cadmium (blue). *E*,  $^1\text{H}$ - $^{15}\text{N}$  HSQC spectrum of cadmium-CmtR with DNA in a 1:1 dimeric protein/DNA ratio. No chemical shift and no variation in signal intensities were observed with respect to the  $^1\text{H}$ - $^{15}\text{N}$  HSQC of free cadmium-CmtR.

metal binding. Structural calculations are consistent with a cadmium-binding site composed of  $\alpha\text{R}$ -associated residues Cys-57, Cys-61, plus Cys-102 of the complementary molecule of the dimer (Fig. 1A).

Our results are therefore consistent with our previous *in vivo* data (16) plus *in vitro* evidence (21) implicating Cys-57 and Cys-61 associated with helix  $\alpha\text{R}$ , plus Cys-102 from the flexible tail, in inducer recognition. The cadmium to sulfur charge transfer band is still observed in our spectra of a C102S mutant, indicative of retention of cadmium binding (supplemental Fig.

S6). Although Cys-57 and Cys-61 thiols are required for CmtR to bind cadmium *in vitro*, the Cys-102 thiol is not, with loss of this side group only reducing the cadmium-affinity by one order of magnitude (21). Thus the Cys-102 thiol presumably is an obligatory ligand for the molecular mechanism but optional for cadmium binding. This implies that binding across the dimeric interface is critical for allostery.

Structures of SmtB and CzrA (13, 17) have visualized a pair of tetradentate zinc-sensing sites at C-terminal  $\alpha 5$  helices, but CmtR has only two (Asp-79 and His-81) potential ligands aligning with those of SmtB and CzrA. When expression from the *cmt* operator-promoter was examined in response to a range of cadmium concentrations in mycobacterial cells containing CmtR mutants it confirmed that Cys-57, Cys-61, or Cys-102 to Ser substitutions rendered the protein fully inducer non-responsive at any cadmium concentration (supplemental Fig. S7). This is consistent with our previous studies of these mutants at a single metal concentration (16) and with the sensory site shown in Fig. 3. Substitutions at Asp-79 and His-81 do not abolish inducer recognition, although they do lessen inducer-mediated de-repression (supplemental Fig. S7). These substitutions do not impair CmtR-mediated repression *in vivo* (supplemental Fig. S7), unlike the elevated constitutive expression detected in cells containing non-functional CmtR mutants (16), confirming that they form stable, folded, and fully functional repressors analogous to the wild type. Investigation of the protonation state of His-81, performed through detection of  $^2\text{J}$

$^1\text{H}$ - $^{15}\text{N}$  couplings, indicates that His-81 exists as an imidazolium in cadmium-CmtR (supplemental Fig. S6) and consequently is not involved in cadmium binding. It is indeed involved in hydrogen bond interactions with Asp-79 of the same subunit and Gln-91 of the other subunit, thus contributing to the stabilization of the dimer interface. In particular, an intramolecular hydrogen-bond between the backbone NH of His-81 and the carboxyl oxygen of Asp-79 is present in more than 25 conformers out of 30 final energy-minimized structures, whereas H $\delta$ 1 of His-81 forms an intermolecular hydrogen bond

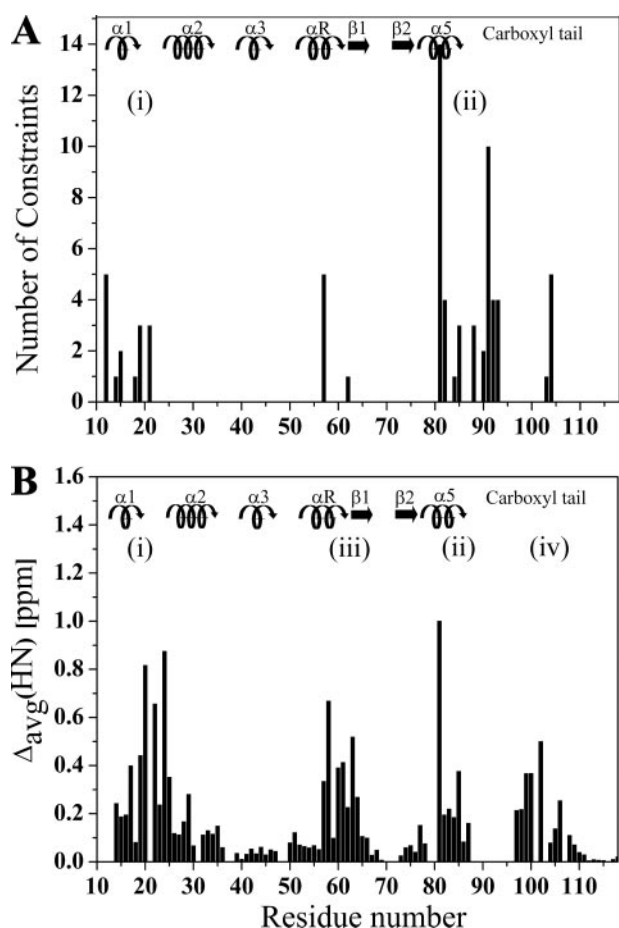


FIGURE 2. **Intersubunit signals and the effects of cadmium.** *A*, number of intersubunit long-range NOEs per residue of dimeric cadmium-CmtR. *B*, the combined chemical shift variation  $\Delta_{\text{avg}}(\text{HN})$  between apo- and cadmium-CmtR (calculated as  $[(\Delta\text{H})^2 + (\Delta\text{N}/5)^2/2]^{1/2}$ , where  $\Delta\text{H}$  and  $\Delta\text{N}$  are chemical shift differences for  $^1\text{H}$  and  $^{15}\text{N}$ , respectively) with secondary structure elements shown above.

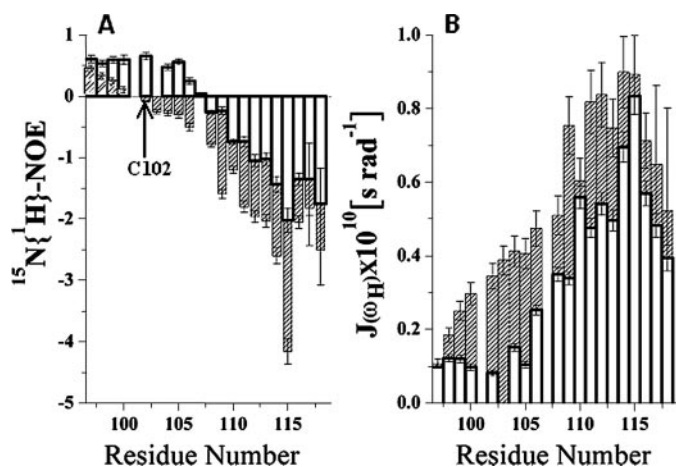


FIGURE 3. **Dynamic properties of the C-terminal tail of CmtR.** *A*, heteronuclear  $^{15}\text{N}\{^1\text{H}\}$ -NOEs of residues 97–118 for apo-CmtR (hashed bars) and cadmium-CmtR (white bars). *B*,  $J(\omega_{\text{H}})$  values of residues 97–118 for apo-CmtR (hashed bars) and cadmium-CmtR (white bars).

with Oe1 of Gln-91 in half of the conformers. The H-bond interactions are further supported by the detection of intersubunit NOEs between the H $\delta$ 2 and H $\epsilon$ 1 of His-81 and the H $\epsilon$ 22 and H $\epsilon$ 21 of Gln-91 in the two-dimensional NOESY spectrum.

**Characterization of Apo-CmtR**—Analysis of the chemical shift index of C $\alpha$ , CO, and C $\beta$  resonances of apo-CmtR (supplemental Table S4) shows that the protein maintains the same secondary structure elements as cadmium-CmtR, consistent with the CD spectra. The NOESY spectra show less than half of the cross-peaks relative to the cadmium derivative, and in general they display lower intensity. After a thorough resonance assignment, it appears that mainly the long range NOEs are lacking even within the secondary structure elements and, dramatically, in the inter-subunit helices  $\alpha$ 1 and  $\alpha$ 5. Particularly, only five intersubunit NOEs are observed at the protein interface, compared with 34 in the cadmium derivative. The few observed NOEs of apo-CmtR are consistent with the overall fold of the cadmium form. The lack of NOEs, together with a normal sub-nanosecond mobility in large parts of the protein as monitored from  $^{15}\text{N}$  relaxation studies (see later), are indicative of large conformational equilibria in the time scale  $10^6$ – $10^3$  s $^{-1}$ . Finally, the disappearance of the NMR signals for residues 88–95, which are part of the interface, show that the apoprotein has a less compact quaternary structure with respect to the cadmium derivative. All of these data suggest, at variance with cadmium-CmtR, that the two molecules sample multiple relative orientations assuming a less defined conformation at the dimer interface.

The analysis of the backbone dynamics of apo-CmtR in the subnanosecond time scale ( $^{15}\text{N}$   $R_1$ ,  $R_2$ , and heteronuclear  $^{15}\text{N}\{^1\text{H}\}$ -NOEs at 312 K) points to a protein of dimeric molecular mass, suggesting the same quaternary structure as cadmium-CmtR, as well as an essentially similar behavior for the large majority of residues between the two proteins, with the exception of the C-terminal region. Apo-CmtR has indeed a highly flexible carboxyl-segment spanning residues 97–118, according to their higher than the average  $J(\omega_{\text{H}})$  values (supplemental Fig. S3) and including the sensory residue Cys-102, which is very mobile as shown by its negative heteronuclear  $^{15}\text{N}\{^1\text{H}\}$ -NOE value (Fig. 3), indicative of fast (nanosecond to picosecond) internal mobility. In cadmium-CmtR, the fast motions of the C-terminal tail are reduced to the segment 106–118 (Fig. 3). Residues 97–105 have indeed  $J(\omega_{\text{H}})$  values largely reduced with respect to the corresponding ones in apo-CmtR (Fig. 3) and on the average value of  $J(\omega_{\text{H}})$  (supplemental Fig. S3). In cadmium-CmtR, Cys-102 is characterized by a positive heteronuclear  $^{15}\text{N}\{^1\text{H}\}$ -NOE and by  $J(\omega_{\text{H}})$  and  $J(0)$  values consistent with the absence of fast and slow backbone motions, respectively (Fig. 3 and supplemental Fig. S4). Thus, metal binding partly organizes and rigidifies a section of the C-terminal tail surrounding the Cys-102 ligand.

$\text{H}_2\text{O}$ - $\text{D}_2\text{O}$  exchange kinetic experiments, performed up to 24 h, strongly support a high degree of conformational equilibria in apo-CmtR, relative to cadmium-CmtR, at the dimer interface. In apo-CmtR 15 residues exchange so fast that their signals in the first  $^1\text{H}$ - $^{15}\text{N}$  HSQC spectra, taken immediately after dissolving the sample in  $\text{D}_2\text{O}$ , are already not detectable, whereas the corresponding signals in cadmium-CmtR decay with half-lives ranging from 1 to 16 h. The rate of exchange depends on the time the NHs are solvent-exposed. Twenty further residues of apo-CmtR have faster (by 2-fold or more) variations of their kinetic constants with respect to cadmium-CmtR. Both classes

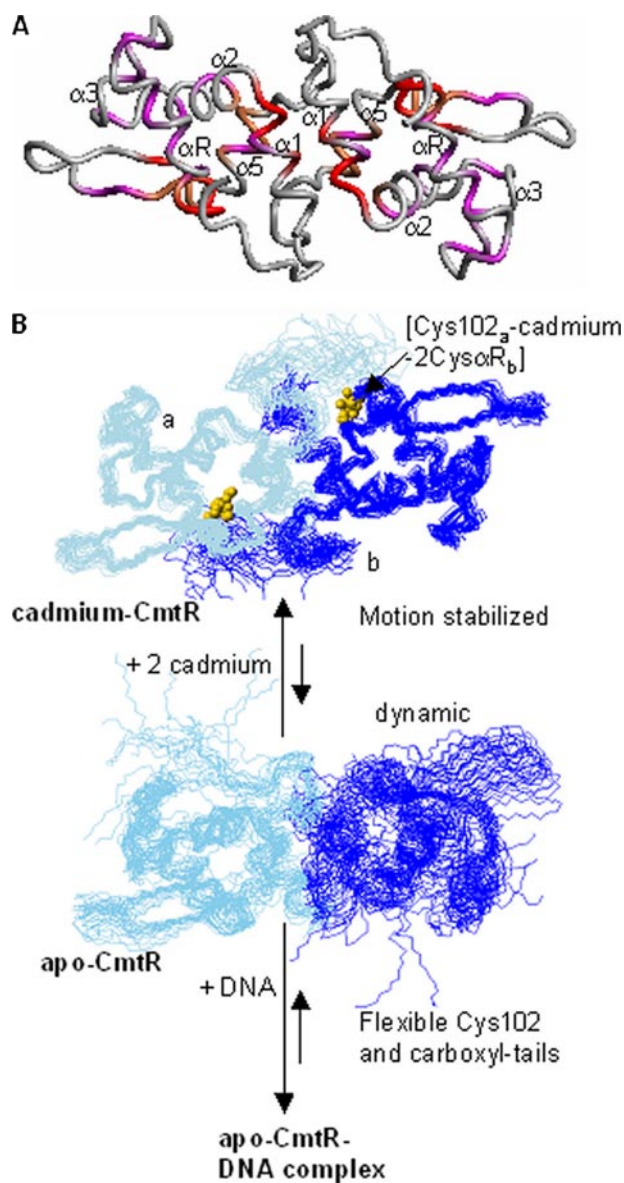


**FIGURE 4. Cadmium-binding dampens mobility.** *A*, ribbon representation of the  $\text{H}_2\text{O}-\text{D}_2\text{O}$  exchange rates of amide protons in apo- versus cadmium-CmtR. The ribbon is color-coded from red to gray, with red representing exchange too fast to be measured in apo-CmtR but slow or non-exchangeable in cadmium-CmtR, orange representing kinetic constants at least 4-fold faster in apo-CmtR, magenta representing 2- to 4-fold faster in apo-CmtR, and gray representing residues with similar behavior in apo- and cadmium-CmtR or not resolved. *B*, the structures and dynamic properties of CmtR. Apo-CmtR is dynamic allowing selection of a conformer with tight affinity for DNA. Cadmium binds via Cys-102 plus two Cys associated with helix  $\alpha\text{R}$  of the other subunit, introducing rigidity, locking the protein into a conformer with weaker affinity for DNA. Cadmium-CmtR is experimentally determined with backbone traces for the thirty lowest energy conformers superimposed. The root mean square deviation to the mean structure of the family considering a single subunit is  $0.87 \pm 0.15 \text{ \AA}$  and  $1.37 \pm 0.14 \text{ \AA}$  for the backbone and the heavy atoms, respectively (root mean square deviation calculated for residues 10–94). If the root mean square deviation is evaluated on the same segment but considering both subunits, the value is  $1.30 \pm 0.40 \text{ \AA}$  and  $1.70 \pm 0.34 \text{ \AA}$ . Apo-CmtR is a structural model obtained by running a CYANA calculation based upon all of the intrasubunit NOEs of cadmium-CmtR, which are all still observable in apo-CmtR, plus the five intersubunit NOEs present in helix  $\alpha 1$  that are also retained in the apo form.

of residue are predominantly located at the dimeric interface (helices  $\alpha 1$  and  $\alpha 5$ ) and at the apo-CmtR binding Cys of helix  $\alpha\text{R}$  (Fig. 4A).

In conclusion, apo-CmtR, while maintaining the same secondary structural elements and the same overall fold, is a flexible protein and lacks a well defined dimer organization. The multiple conformations sampled by the protein weaken the NOEs until they eventually disappear, particularly those at the dimer interface. This is therefore the best structural and dynamical characterization we can achieve in solution. Furthermore, a flexible protein has very low tendency to crystallize, and, in the event that it does, it would result in the potentially misleading selection of a single conformer. The resulting picture is of a protein that has reasonably well defined secondary structural elements, but with a tertiary structure that is dynamic among widely different conformational arrangements. Analogous behavior was observed in the superoxide dismutase-like protein from *Bacillus subtilis* (36), where its NMR properties indicate a conformational mobility for most of the protein, characterized by defined secondary-structure elements and a dynamic tertiary structure. In contrast, the x-ray crystal structure of the same protein shows a well ordered tertiary structure. The different dynamic properties of apo- with respect to cadmium-CmtR reveal a mechanism by which cadmium binds to ligands from either side of the subunit interface and, aided by the coincident formation of inter- and intra-subunit hydrogen bonds, locks the dimer into less mobile forms.

*Cadmium Inhibition of CmtR DNA Binding Observed by NMR*—Addition of DNA to apo-CmtR (at mM concentration) causes NH cross-peaks to disappear in the  $^1\text{H}-^{15}\text{N}$  HSQC experiments with the notable exception of residues 98–118 from the C-terminal tail (Fig. 1B). Fig. 1C shows the slope of signal disappearance, which is consistent with the exclusive formation of three protein dimers per DNA fragment at the present concentrations. This is not inconsistent with the previous proposal of 1:1, 1:2 and 1:3 species at much lower concentrations (21). The disappearance of the NH signals is due to the formation of the large molecular mass DNA-protein complex, as previously observed by electrophoretic mobility shift assays (16) and by fluorescence anisotropy at elevated protein concentrations (21), and/or due to the occurrence of chemical exchange phenomena, which leads to line broadening. An exception is the flexible unstructured C-terminal tail, which reorients faster than the overall tumbling rate in apo-CmtR and maintains the same properties in the apo-CmtR-DNA complex. This is also indicated by the backbone NH chemical shifts continuing to resonate in the typical region of unstructured proteins (Fig. 1B) and by the presence of negative heteronuclear  $^{15}\text{N}\{^1\text{H}\}$ -NOE values even in the large apo-CmtR-DNA complex. Similar chemical shift values for the C-terminal region in both apo-CmtR and apo-CmtR-DNA indicate that no significant conformational changes occur in this region including the ligand Cys-102. Metal-mediated impaired binding of CmtR to DNA was then examined *in vitro* via NMR by titrating the apo-CmtR-DNA mixture with cadmium chloride. Addition of up to 1 cadmium equivalent to dimeric apo-CmtR-DNA mixture caused the re-appearance of NH cross-peaks in  $^1\text{H}-^{15}\text{N}$  HSQC spectra from regions other than the carboxyl-tail (Fig. 1D). Fig. 1E shows the  $^1\text{H}-^{15}\text{N}$  HSQC of cadmium-CmtR-DNA mixture in a 1:1 dimeric protein-DNA ratio obtained by mixing pre-formed cadmium-CmtR to DNA. No chemical shift and no var-

iation in signal intensities are observed with respect to the  $^1\text{H}$ - $^{15}\text{N}$  HSQC of free cadmium-CmtR. Therefore, we can safely conclude that (i) cadmium ions dissociate apoprotein from DNA and (ii) cadmium-loaded CmtR does not bind DNA.

## DISCUSSION

CmtR is arranged in dimers where each subunit shares the typical fold of this family of metal-responsive transcriptional repressors but with the additional features of the metal-binding site associated with  $\alpha\text{R}$  and an unstructured carboxyl-tail (Fig. 1A). Binding of cadmium reduces the conformational heterogeneity of regions within the CmtR subunits and locks the two subunits into a better defined reciprocal orientation (Fig. 4). This produces a change in conformational heterogeneity experimentally supported by a dramatic reduction of  $\text{H}_2\text{O}$ - $\text{D}_2\text{O}$  exchange rates, most notably at the dimer interface, in cadmium-CmtR compared with apo-CmtR (Fig. 4A) and by a dramatic increase of the number of NOEs. The cadmium-binding sites bridge the homo-dimers by exploiting Cys-102 from one subunit in association with Cys-57 and Cys-61 from the other (Fig. 1A). DNA associates with the apo form but not the cadmium-bound form. Our NMR studies confirm that three apo dimeric proteins bind one DNA molecule (21) and show that the cadmium-loaded form does not interact with DNA under any ratio. In essence, DNA can select an optimal conformer from a pool of dynamic apo-homo-dimers, but cadmium drives the two subunits into a more rigid conformation, both at the tertiary and quaternary level, which excludes the preferred partners for DNA (Fig. 4B).

Most of the metal-sensing sites described in ArsR/SmtB family members involve ligands from both subunits at  $\alpha 3$  and/or  $\alpha 5$  positions (8). In CmtR, however, the metal sensory site is provided by cysteines belonging to  $\alpha\text{R}$ . Diversity may also exist in the allosteric mechanisms of different family members. Comparison of the crystal structures of apo and zinc forms of SmtB identified a regulatory hydrogen-bond network connecting a sensory residue at helix  $\alpha 5$  to DNA-associating  $\alpha\text{R}$ , solely when metal is bound (17). Importantly,  $\text{H}_2\text{O}$ - $\text{D}_2\text{O}$  exchange rates of CzrA suggested that zinc-binding reduced the internal dynamics of this protein (17). Evidence supporting metal-mediated structural stabilization has also been obtained for MntR and DtxR (37, 38). However, these two proteins show enhanced repression in the metal-bound forms, opposite to ArsR/SmtB, hence metal association must favor the conformers of MntR and DtxR that bind most tightly to DNA.

The high degree of flexibility in the apo form of the C-terminal region containing Cys-102 raises the intriguing possibility that Cys-102 protrudes and acts in the recruitment of cadmium to the sensory site. The sources of metal for metal sensors are unknown. One model proposes that some metals are not freely released into the cell (39–42) but passed to their destinations by ligand-exchange from, for example, metallochaperones or metal importers. Under this regime, consistent with documented roles for unfolded regions in macromolecular interactions (43, 26), the carboxyl-tail in apo-CmtR would acquire cadmium from a donor. Accordingly, the reported (21)  $1.7 \times 10^{12} \text{ M}^{-1}$  affinity of CmtR for cadmium is very high. This will for-

mally allow a cell to detect toxic cadmium at nanomolar concentrations, at least as low as an atom per cell volume. Most importantly, the molecular mechanism by which CmtR binds cadmium to quench protein dynamics and thereby inhibit DNA association (Fig. 4B) is apparent from the data reported here, which show that the distribution of protein conformations is reduced when cadmium binds.

## REFERENCES

- Bertini, I., Sigel, A., and Sigel, H. (2001) *Handbook on Metalloproteins*, 1 Ed., Marcel Dekker, New York
- Rutherford, J. C., and Bird, A. J. (2004) *Eucaryotic Cell* **3**, 1–13
- Heuchel, R., Radtke, F., Georgiev, O., Stark, G., Aguet, M., and Schaffner, W. (1994) *EMBO J.* **13**, 2870–2875
- Selvaraj, A., Balamurugan, K., Yepiskoposyan, H., Zhou, H., Egli, D., Georgiev, O., Thiele, D. J., and Schaffner, W. (2005) *Genes Dev.* **19**, 891–896
- Huckle, J. W., Morby, A. P., Turner, J. S., and Robinson, N. J. (1993) *Mol. Microbiol.* **7**, 177–187
- Wu, J., and Rosen, B. P. (1993) *J. Biol. Chem.* **268**, 52–58
- Endo, G., and Silver, S. (1995) *J. Bacteriol.* **177**, 4437–4441
- Pennella, M. A., and Giedroc, D. P. (2005) *Biomaterials* **18**, 413–428
- Turner, J. S., Morby, A. P., Whitton, B. A., Gupta, A., and Robinson, N. J. (1993) *J. Biol. Chem.* **268**, 4494–4498
- Blindauer, C. A., Harrison, M. D., Parkinson, J. A., Robinson, A. K., Cavet, J. S., Robinson, N. J., and Sadler, P. J. (2001) *Proc. Natl. Acad. Sci. U. S. A.* **98**, 9593–9598
- Shi, W., Wu, J., and Rosen, B. P. (1994) *J. Biol. Chem.* **269**, 19826–19829
- Turner, J. S., Glands, P. D., Samson, A. C., and Robinson, N. J. (1996) *Nucleic Acids Res.* **24**, 3714–3721
- Cook, W. J., Kar, S. R., Taylor, K. B., and Hall, L. M. (1998) *J. Mol. Biol.* **275**, 337–346
- VanZile, M. L., Cospers, N. J., Scott, R. A., and Giedroc, D. P. (2000) *Biochemistry* **39**, 11818–11829
- Cavet, J. S., Meng, W., Pennella, M. A., Appelhoff, R. J., Giedroc, D. P., and Robinson, N. J. (2002) *J. Biol. Chem.* **277**, 38441–38448
- Cavet, J. S., Graham, A. I., Meng, W., and Robinson, N. J. (2003) *J. Biol. Chem.* **278**, 44560–44566
- Eicken, C., Pennella, M. A., Chen, X., Koshlap, K. M., VanZile, M. L., Sacchettini, J. C., and Giedroc, D. P. (2003) *J. Mol. Biol.* **333**, 683–695
- Ye, J., Kandedgedara, A., Martin, P., and Rosen, B. P. (2005) *J. Bacteriol.* **187**, 4214–4221
- Harvie, D. R., Andreini, C., Cavallaro, G., Meng, W., Connolly, B. A., Yoshida, K., Fujita, Y., Harwood, C. R., Radford, D. S., Tottey, S., Cavet, J. S., and Robinson, N. J. (2006) *Mol. Microbiol.* **59**, 1341–1356
- Pennella, M. A., Arunkumar, A. I., and Giedroc, D. P. (2006) *J. Mol. Biol.* **356**, 1124–1136
- Wang, Y., Hemmingsen, L., and Giedroc, D. P. (2005) *Biochemistry* **44**, 8976–8988
- Sambrook, J. R., and Russell, D. W. (2001) *Molecular Cloning: A Laboratory Manual*, Cold Spring Harbor Laboratory Press, New York
- Pelton, J. G., Torchia, D. A., Meadow, N. D., and Roseman, S. (1993) *Protein Sci.* **2**, 543–558
- Gagne, R. R., Tsuda, S., Li, M. X., Chandra, M., Smillie, L. B., and Sykes, B. D. (1994) *Protein Sci.* **3**, 1961–1974
- Guntert, P. (2004) *Methods Mol. Biol.* **278**, 353–378
- Anderluh, G., Gokce, I., and Lakey, J. H. (2004) *J. Biol. Chem.* **279**, 22002–22009
- Arseniev, A., Schultze, P., Wörgötter, E., Braun, W., Wagner, G., Vasak, M., Kägi, J. H., and Wüthrich, K. (1988) *J. Mol. Biol.* **201**, 637–657
- Vriend, G. (1990) *J. Mol. Graphics* **8**, 52–56
- Laskowski, R. A., Rullmann, J. A. C., MacArthur, M. W., Kaptein, R., and Thornton, J. M. (1996) *J. Biomol. NMR* **8**, 477–486
- Farrow, N. A., Muhandiram, R., Singer, A. U., Pascal, S. M., Kay, C. M., Gish, G., Shoelson, S. E., Pawson, T., Forman-Kay, J. D., and Kay, L. E. (1994) *Biochemistry* **33**, 5984–6003
- Grzesiek, S., and Bax, A. (1993) *J. Am. Chem. Soc.* **115**, 12593–12594
- Peng, J. W., and Wagner, G. (1992) *J. Magn. Reson.* **98**, 308–332

## Structure-Function Analysis of CmtR

33. Tjandra, N., Feller, S. E., Pastor, R. W., and Bax, A. (1995) *J. Am. Chem. Soc.* **117**, 12562–12566
34. Riek, R., Pervushin, K., and Wüthrich, K. (2000) *Trends Biochem. Sci.* **25**, 462–468
35. Aravind, L., Anantharaman, V., Balaji, S., Babu, M. M., and Iyer, L. M. (2005) *FEMS Microbiol. Rev.* **29**, 231–262
36. Banci, L., Bertini, I., Calderone, V., Cramaro, F., Del Conte, R., Fantoni, A., Mangani, S., Quattrone, A., and Viezzoli, M. S. (2005) *Proc. Natl. Acad. Sci. U. S. A.* **102**, 7541–7546
37. Rangachari, V., Marin, V., Bienkiewicz, E. A., Semavina, M., Guerrero, L., Love, J. F., Murphy, J. R., and Logan, T. M. (2005) *Biochemistry* **44**, 5672–5682
38. Golymskiy, M. V., Davis, T. C., Helmann, J. D., and Cohen, S. M. (2005) *Biochemistry* **44**, 3380–3389
39. Outten, C. E., and O'Halloran, T. V. (2001) *Science* **292**, 2488–2492
40. Finney, L. A., and O'Halloran, T. V. (2003) *Science* **300**, 931–936
41. Changela, A., Chen, K., Xue, Y., Holshen, J., Outten, C. E., O'Halloran, T. V., and Mondragon, A. (2003) *Science* **301**, 1383–1387
42. Banci, L., and Rosato, A. (2003) *Acc. Chem. Res.* **36**, 215–221
43. Wright, P. E., and Dyson, H. J. (1999) *J. Mol. Biol.* **293**, 321–331

